

GALVANIC CORROSION OF CARBON AND STEEL IN AGGRESSIVE ENVIRONMENTS

By Mohammadreza Tavakkolizadeh,¹ Student Member, ASCE,
and Hamid Saadatmanesh,² Member, ASCE

ABSTRACT: The demand for the use of carbon-fiber-reinforced plastics (CFRP) in rehabilitation of deteriorating infrastructure is increasing worldwide. The design characteristics of reinforced concrete or steel members can be enhanced significantly by epoxy bonding CFRP laminates to the critically stressed tension areas. There is, however, a concern regarding possible galvanic corrosion when carbon and steel are bonded together. This paper presents the result of a study on the galvanic corrosion between CFRP laminates and steel. A total of 38 specimens made of steel and carbon fibers were prepared and tested. Two simulated aggressive environments and three different amounts of epoxy coating were used in addition to samples with no coating at all. Furthermore, the effect of the sizing agent on the galvanic corrosion rate was investigated, and three different solvents were used to remove the sizing agents from the surface of the carbon fibers. Potentiodynamic polarization and galvanic corrosion tests were conducted. The results of the experiments showed the existence of galvanic corrosion; however, the rate of such corrosion could be decreased significantly by epoxy coating.

INTRODUCTION

The status of the country's deteriorating infrastructure received national attention when, more than three decades ago, the Silver Bridge on the Ohio River in West Virginia suddenly collapsed. Before 1967, there were no mandatory inspection and control of bridges. Since then, the American Association of State Highway and Transportation Officials (AASHTO) and the Federal Highway Administration (FHWA) have adopted programs to rate bridges on the nation's highways through biannual inspection. As a result, it has been found that more than one third of the highway bridges in the United States can be considered substandard (Klaiber et al. 1986). According to the National Bridge Inventory (NBI) update in 1998, the number of substandard highway bridges in this country is more than 172,600. It is noted that this figure does not even include railroad and pedestrian bridges (FHWA 2000).

The cost for rehabilitation and repair in most cases is far less than the cost of replacement. Furthermore, repair and rehabilitation usually take less time than replacement, reducing service interruption time. Considering the limited resources available to mitigate this problem, it would be prudent to explore new materials and adopt cost-effective techniques to address this important issue. The primary reasons for deterioration of the bridges include corrosion, fatigue, increase in dead load, and permitted live load.

Corrosion is among the major factors affecting the long-term serviceability of these types of bridges, particularly those located in cold regions where deicing salts and other aggressive chemicals are used. The reduction of the cross-sectional area of a bridge member caused by oxidation decreases the load-carrying capacity of that member. Corrosion can also occur as a result of galvanic action. Any nonuniformity in the material can develop a corrosion cell and accelerate the deterioration process. The latter problem is more critical in connections and cover plates if different plate materials are used.

The observation of fatigue cracking of steel bridges since

1967, especially in cold regions, has shown that old steel bridges have major fatigue problems. The lack of quality control of the welds, rivets, and bores and the introduction of large initial discontinuities are among the important issues affecting the fatigue life of these structures. The use of several low-fatigue-resistant details by designers and the lack of knowledge in fracture mechanics has compounded this problem. The low-temperature environments that most of these bridges are subjected to decrease the fracture toughness of steel and can cause brittle failure.

After years of service, the dead weight of a bridge usually increases due to several factors. These may include the widening of the roadway, the addition of a bike lane or pedestrian walkway, resurfacing of the road, or increasing the grade to overcome the settlement of the aging bridge. Most of the conventional repair techniques can also increase the dead weight of the structures significantly. The extra dead weight will increase the stress level in all the members and intensify the problems stated above.

STRENGTHENING WITH FIBER-REINFORCED COMPOSITES

The significant advancements in materials science during the Cold War, and the increasing applications of these materials for civilian purposes, have brought about new opportunities to address the problems of aging bridges. In particular, fiber-reinforced plastic (FRP) materials have been used successfully in a number of repair and rehabilitation applications. The excellent tensile and fatigue strength, light weight, and high corrosion resistance of these materials makes them an attractive candidate for structural application in substandard steel bridges.

An effective technique for upgrading existing steel girders involves epoxy bonding of carbon-fiber-reinforced plastic (CFRP) plates or laminates to the tension flange of the girder to increase the load-carrying capacity and fatigue strength. Since no welding is required, the addition of CFRP plates does not decrease the fatigue strength of the girder. By reducing the stress level in the girder, the fatigue life of the structure will in fact be increased. The CFRP can also be used as a patch for the arrest of cracks caused by fatigue. CFRP costs more than steel, yet despite this higher cost, savings in labor, machinery, and application time (traffic interruption) make this method economically very attractive. The fact that CFRP is corrosion resistant minimizes the need for regular maintenance and painting. Meanwhile, low weight and small thickness pre-

¹Res. Assoc., Dept. of Civ. Engrg. and Engrg. Mech., Univ. of Arizona, Tucson, AZ 85721.

²Prof., Dept. of Civ. Engrg. and Engrg. Mech., Univ. of Arizona, Tucson, AZ 85721.

Note. Discussion open until January 1, 2002. To extend the closing date one month, a written request must be filed with the ASCE Manager of Journals. The manuscript for this paper was submitted for review and possible publication on May 15, 2000; revised October 23, 2000. This paper is part of the *Journal of Composites for Construction*, Vol. 5, No. 3, August, 2001. ©ASCE, ISSN 1090-0268/01/0003-0200-0210/\$8.00 + \$.50 per page. Paper No. 22176.

vent any substantial increase in dead weight and loss in bridge clearance.

There is, however, a major issue concerning this strengthening technique: the possibility of galvanic corrosion between carbon and steel. In this study, the galvanic corrosion between steel and a CFRP sheet will be investigated. Since carbon fibers have metallic characteristics, the steel-carbon system may have a tendency to form a galvanic cell, and corrosion can occur at a higher rate. In order to investigate the possibility and intensity of galvanic corrosion, four different CFRP samples with different amounts of epoxy cover ranging from bare fibers to full coverage with resin were tested in seawater and deicing solution. Different solutions were also used to remove sizing agents from the surface of loose carbon fibers. As a result of this study, a better understanding of the galvanic corrosion behavior of the CFRP-steel system can be achieved.

PREVIOUS WORKS

Strengthening Steel Girders with CFRP Laminates

The focus of this study is on epoxy-bonded sheets or plates as a means of strengthening steel beams. A literature survey revealed several studies on the use of epoxy-bonded steel plates for strengthening steel and concrete structures. The field application of this technique, however, has been limited to only concrete structures. The first recorded application of this technique can be dated as far back as 1964 in Durban, South Africa, where the reinforcement in a beam was accidentally left out during the construction (Dussek 1980). This beam was strengthened by bonding steel plates to the tension area. By 1975, more than 200 defective slabs of an elevated motorway in Japan had been strengthened with this technique (Raithby 1980).

In a study conducted at Case Western Reserve University (Nara and Gasparini 1981) and the University of Maryland (Albrecht et al. 1984), adhesive bonding and end bolting of steel cover plates to steel girders provided a substantial improvement in the fatigue life of the system. By a more uniform stress transfer to the plate through the epoxy layer, stress concentrations were significantly reduced. The studies indicated that the use of adhesive bonding with end bolting could increase the fatigue life of the system by a factor of 20, compared to the traditional welded cover plates.

Knowing the advantages of epoxy-bonded plates, the next evolutionary step in this technology was the utilization of high-performance advanced composite laminates in lieu of steel plates. The light weight and corrosion resistance of these materials make them attractive alternatives for this application. Glass-fiber-reinforced plastic (GFRP) sheets have been used in strengthening of reinforced concrete and masonry structures for the past decade. In the case of concrete beams, significant reduction in cracking was observed, and in some cases the ultimate strength of the beam was enhanced by up to four times that of the original beam (Saadatmanesh and Ehsani 1991). Using composite jackets for retrofitting concrete columns has led to significant improvements in ductility (Saadatmanesh et al. 1997). Recently, the potential of advanced composites for the rehabilitation of unreinforced masonry walls was investigated. The results have shown a significant improvement in the ductility and strength of the retrofitted walls (Saadatmanesh 1994).

During the past decade, only a few studies have been reported on the use of FRP plates for strengthening steel beams. The significant difference in this approach is the need for higher-modulus composites. CFRP is a good candidate for this application. The possibility of using CFRP in repair of steel-concrete composite bridges was investigated by Sen and Liby (1994), who tested a total of six specimens with yield strengths

of 310 and 370 MPa. For each yield strength, there were one control, one 2-mm retrofit, and one 5-mm retrofit. Each specimen was 6.10 m long and consisted of a $W8 \times 24$ steel section attached to a 71.1 cm wide by 11.5 cm thick concrete slab through welded shear connectors. The beams were loaded in flexure to yielding of their tension flanges and then were repaired with 3.65 m long, 15 cm wide, and either 2 or 5 mm thick, epoxy-bonded CFRP laminates. Sen and Liby concluded that the CFRP laminates could considerably improve the ultimate capacity of the composite beams regardless of the yield strength of the steel. Average increases in the ultimate capacity of 11 and 50% were reported for 2 and 5 mm CFRP laminates, respectively. They also emphasized the need for further research on the effect of moisture and humidity on the long-term durability of the system and the possibility of galvanic corrosion.

In another study, Mertz and Gillespie (1996) investigated the advantages of using advanced materials in the rehabilitation of deteriorated steel bridges. In their small-scale tests, they retrofitted eight 1.52 m long $W8 \times 10$ steel beams with a yield strength of 250 MPa using five different retrofitting schemes. They reported an average 60% increase in strength for carbon-retrofitted specimens. They also concluded that in order to avoid the possibility of galvanic corrosion, an electrically insulating layer of composite, such as GFRP, can be placed between CFRP and steel.

Galvanic Corrosion

The use of carbon-fiber composites with steel structures requires a thorough understanding of the phenomenon of galvanic corrosion. In theory, as long as two materials have not contacted each other, a corrosion cell will not initiate. However, in case of direct contact between carbon fibers and steel in the presence of an electrolyte, the wet corrosion cell could accelerate the corrosion of steel and create possible blistering and subsequent delamination or debonding.

Tucker and Brown (1989) studied the possibility of galvanic corrosion for graphite/epoxy and graphite/vinyl ester composites directly coupled with mild steel in seawater. The graphite/vinyl ester specimens were 20.3 cm long by 13 mm wide by 9.5 mm thick. The graphite/epoxy specimens were 214 cm long by 13 mm wide by 6.4 mm thick. They reported a significant blistering in vinyl ester-based composites after 6 months. These blisters occurred in a regular pattern that coincided with the fiberglass tows used in the graphite fabric. They noted that the epoxy-based composites did not show any sign of blistering due to the absence of glass tows or the use of epoxy (nonhydrolyzable matrix). They concluded that the diffusion of water into the composite and migration of water-soluble molecules within the composite were the main reasons for the initiation of blisters, and the osmotic pressure caused continuous growth of the blisters.

Sloan and Talbot (1992) investigated the galvanic coupling of graphite/epoxy composites and magnesium in seawater. All specimens were cut from a 26-ply T-300 graphite epoxy laminate with two fiberglass surface plies. Specimens were then cut into $90 \times 13 \times 3.6$ mm coupons. In order to measure the effect of galvanic corrosion on the shear strength, four-point bending tests were performed with span-to-depth ratio (L/h) of 2 to ensure interlaminar shear failure. Sloan and Talbot observed a 30% decrease in the shear strength of the composite coupled with magnesium after 140 days of exposure to seawater. They concluded that, in a marine environment, no epoxy that contains hydrolyzable linkage such as ester bonds should be used where metal coupling could be likely. They also suggested that the simplest way to prevent galvanic coupling is electrical isolation of carbon fibers and metal by using organic fiber plies and sealer coatings.

Cetin et al. (1998) investigated the corrosion of rebars in reinforced concrete members with externally bonded CFRP in

seawater. In addition to testing Forca C1-30 carbon fibers, they also tested solid graphite rods that had no sizing agents. Sizing agents are chemical compounds that are mainly applied to the surface of the fibers during manufacturing in order to protect them during handling and to enhance the fiber/matrix adhesion. Grade 60 rebar was also used in their study. They conducted separate polarization tests on graphite rods, carbon fibers, and steel rebars. It was observed that the corrosion rate of graphite rod was 10 times higher than that of the carbon fibers. An attempt to remove the sizing agents from the surface of the fibers using acetone and ultrasonic cleaner was not very successful, and the corrosion rate of fibers remained lower than the graphite rod as a result of the presence of sizing agents on the surface of fibers. After considering the coupling effect, they concluded that while the steel rebar showed accelerated corrosion in the presence of the graphite rod, the sizing agents on carbon fibers decreased the galvanic corrosion rate significantly.

GALVANIC CORROSION

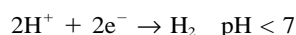
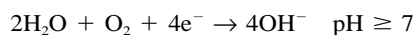
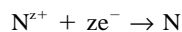
Theory

Corrosion has been defined as “degradation of a metal by an electrochemical reaction with its environment” (Trethewey and Chamberlain 1988). It is always easier to explain the phenomenon in a basic wet corrosion cell such as that shown in Fig. 1, which has four essential components: the anode, cathode, electrolyte, and electrical connection. In the absence of any one of these components, the corrosion reaction will stop. A brief description of each of these components is given below.

- Anode: location where corrosion of metal takes place. The metal loses electrons and becomes the ion in the solution, or it may form an insoluble product.



- Cathode: part that usually attracts the electrons created in the anode. The electrons are consumed by the reactions at the cathode. Such reactions can be the formation of a metal film, reduction of oxygen, or evolution of hydrogen.



- Electrolyte: solution with sufficient conductivity for transferring the ions.
- Electrical connection: connection necessary between the

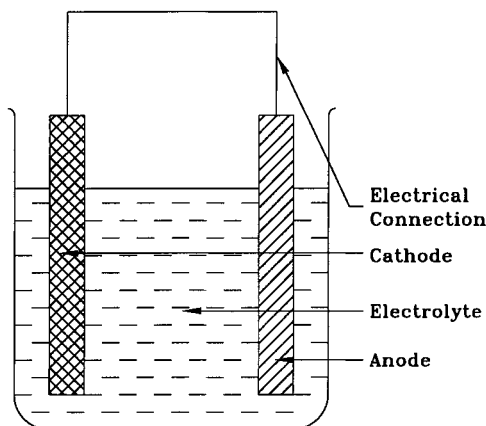


FIG. 1. Schematic of Basic Wet Corrosion Cell

anodic and cathodic sites for corrosion to take place. In cases in which the anode and cathode are not part of the same material, a physical connection is necessary for the current to flow and the corrosion to occur.

The potential difference between the two electrodes can be readily measured. In order to establish an absolute value for the potential of each material, the potential difference between the material and the standard hydrogen electrode (SHE), with the potential of zero volts at 25°C, can be measured and referred to as the standard reduction potential. Since use of the SHE in routine laboratory tests is difficult, other reference electrodes have been used.

The most commonly used reference electrode is the standard calomel electrode (SCE), with a potential of +0.242 V versus SHE at 298°K. The SCE consists of a platinum wire in contact with mercury (Hg) and mercury chloride (HgCl), which is held in a glass tube plugged by a porous material. The tube is then placed inside a larger tube containing saturated potassium chloride (KCl) with another porous plug at the end, as shown in Fig. 2. Porous plugs allow the passage of ions without significant cross contamination.

The flow of current I (in amperes, A) provides a clear indication of an active corrosion process. To eliminate the effect of the relative size of the electrodes, the current density, i (A/m^2), is used as the true indication of the corrosion rate. Faraday's law of electrolysis and the corrosion current density can be used to evaluate the mass lost in the corrosion process.

Polarization is an important corrosion evaluation method. It

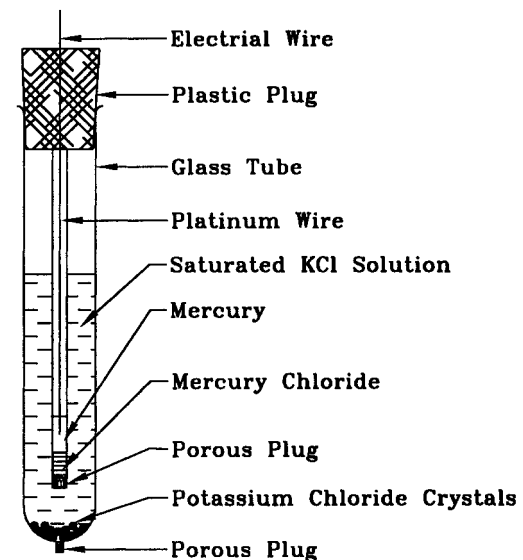


FIG. 2. Schematic of Saturated Calomel Electrode (SCE)

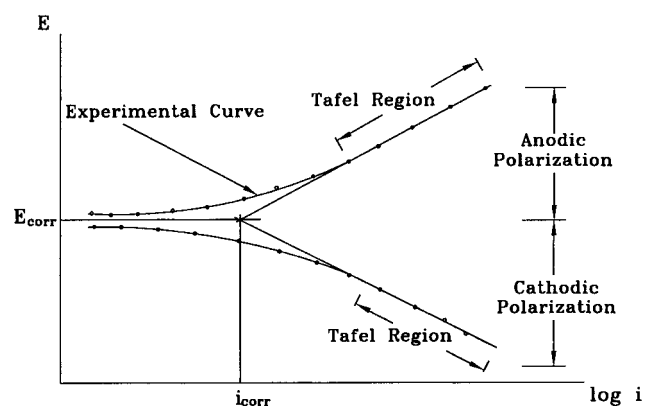


FIG. 3. Typical Polarization Result Showing Tafel Extrapolation

evaluates the electrochemical response as the potential of a material is made to deviate from its steady-state value under freely corroding conditions, E_{corr} , called the free corrosion potential. Polarization can be cathodic or anodic, and it has been shown that the true response, when plotted as potential versus $\log i$, can be idealized as two straight lines intersecting at a point that corresponds to the corrosion current density of the material. The plot that contains these two lines is referred to as the Tafel plot (Fontana 1987). Usually the extrapolation of the linear portion of the Tafel plot obtained from tests will result in the estimation of corrosion current density, i_{corr} , as shown in Fig. 3.

Potentiodynamic Polarization Test

The polarization test is performed to investigate the corrosion properties of a material in a certain solution. This test provides not only an estimate of the corrosion rate of a material in a solution, but also can be used for the assessment of the galvanic corrosion rate of two materials coupled together. During this test, the potential difference between the material and the reference electrode is monitored, as well as the current. In the polarization test setup, a reference electrode and the working electrode (material under study) are connected via a high impedance voltmeter. A counterelectrode (usually platinum, Pt) is connected to the working electrode via a galvanometer and a variable voltage source (potentiostat), as shown in Fig. 4. Using a working electrode with an exposed area of 1 cm^2 would facilitate the analysis.

The three electrodes are then placed in a glass container filled with the solution under study. For solutions with a relatively low conductivity, the reference and working electrodes are placed as close as possible to each other to prevent any possible potential drop. In this experiment, by changing the current between the counter- and the working electrodes, different potentials will be induced between the reference and the working electrodes. A polarization plot can be obtained by scanning from some potential below the free corrosion potential to some potential above it. Each plot will have two branches, one corresponding to the cathodic polarization (below E_{corr}), and the other to the anodic polarization (above E_{corr}).

The corrosion current density of the coupled system can be predicted by superimposing the polarization plots of two different materials in one graph. Such a plot is commonly referred to as the Evans diagram (Fontana 1987). Usually more than one cathodic and anodic reaction occurs in a system. For example, hydrogen evolution can occur on both electrodes, both electrodes can corrode, and more than one corrosion product can be developed. The Evans diagram can also be used to predict the overall corrosion rate of a system.

Galvanic Corrosion Test

The Evans diagram discussed above does not directly evaluate the interaction between the two metals in the solution. Another method for evaluating galvanic corrosion is the direct galvanic coupling test. In this technique, no external potential or current is applied, and the current or potential of a system consisting of two different materials inside a solution is monitored. In other words, the two materials replace the working and counterelectrodes of the previous method and are connected to each other via a galvanometer. A reference electrode is then connected to each electrode during the test in order to monitor the potential difference between the electrodes, as shown in Fig. 5. Testing will continue until a constant current or identical potentials between the cathode and the anode is achieved.

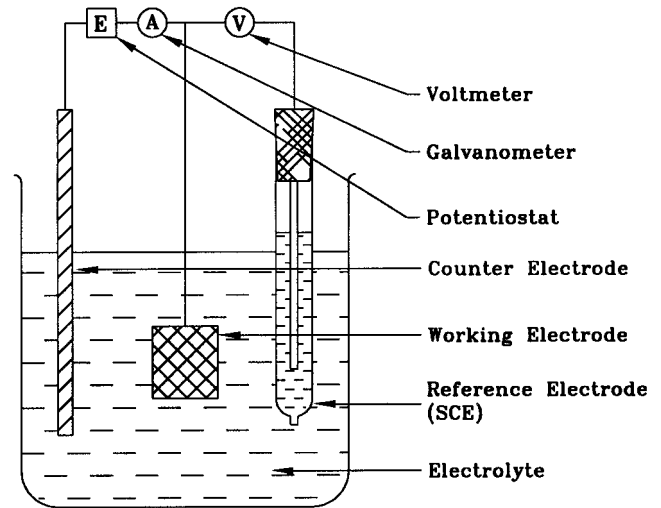


FIG. 4. Schematic of Electrical Circuitry for Polarization Measurement

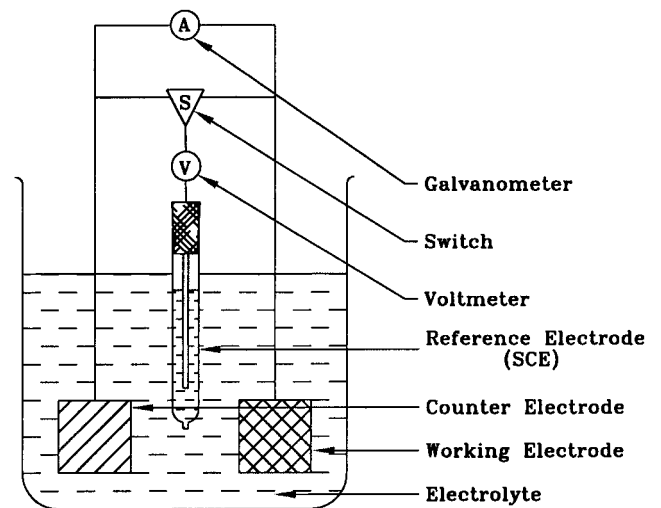


FIG. 5. Schematic of Electrical Circuitry for Galvanic Coupling Measurement

EXPERIMENTAL STUDY

In order to investigate the galvanic corrosion between carbon and steel and to evaluate the galvanic corrosion rate, two different experiments were adopted. Carbon fibers washed in different solvents and tested in different electrolytes were considered in this study. Corrosion current density obtained from each experiment is an important parameter directly related to the corrosion rate. Comparison between the corrosion rates of samples with different thicknesses of epoxy coating in different electrolytes provides a thorough understanding of the phenomenon and assists in developing techniques to eliminate the galvanic corrosion problem.

Test Variables

The effects of several parameters on the corrosion rate of the CFRP/steel system were considered. Two simulated aggressive environments were considered: seawater and a deicing salt solution. As was indicated before, the epoxy coating of carbon fibers plays an important role in the galvanic corrosion process. Therefore, four different types of coupons were made with different amounts of coatings. In order to minimize the effect of sizing agents by removing them, three different solutions were used: acetone, isopropyl alcohol, and carbon tetrachloride. The as-received fibers are then used as control specimens in the test matrix.

Materials

A two-component *epoxy* was used for preparing the CFRP coupons. The mixing ratio of the epoxy was two parts resin (bisphenal A based) to one part hardener (polyamine based) by volume. The epoxy had a pot life of 45 min and a fully cured time of 7 days at 25°C.

A unidirectional *carbon fabric* (680 g/m²), T-300-12K/sticky string style, was used in this study. Carbon fibers were PAN based (made from polyacrylonitrile precursor), with ultimate tensile strength of 3,500 MPa and tensile modulus of 230 GPa. Small coupons with dimensions of 2 × 2 cm were made on glass sheets to assure a flat surface and to prevent the leakage of electrolyte during the experiments. Four different thicknesses of epoxy cover were considered for the carbon fibers, as shown in Fig. 6: (a) fabric without any epoxy cover, (b) fabric with a thin layer of epoxy on the back side, (c) fabric saturated with a thin film of epoxy, and (d) fabric saturated and covered with an amount of epoxy typical of that used in the wet layup system in the field.

Solvents were used to remove any existing coating and sizing in order to minimize the effect of sizing agents on the results. Acetone, isopropyl alcohol, and carbon tetrachloride were the three solvents used in the study. Before each carbon sample was prepared, the loose fibers were soaked in these solutions for 12 h. Then, they were washed with fresh solutions and left to dry out.

Mild 6 mm thick A36 *steel* plates were used. The plates were cut in 2 × 2 cm pieces and sanded with grit 80 and 150 sand paper before each experiment.

Substitute ocean water with an approximate pH of 7.25 was used as one of the two *electrolytes*, following ASTM D1141, (ASTM 1999). The major components of the solution were NaCl (24.53 g/L), MgCl₂ (5.20 g/L), Na₂SO₄ (4.09 g/L), CaCl₂ (1.16 g/L), KCl (0.695 g/L), and NaHCO₃ (0.201 g/L). Deicing salt solution was used as the second electrolyte in this study. This solution was prepared by using NaCl and CaCl₂ with the ratio of 2:1. The solution had a 7% concentration of salt by weight with a pH of 7.90.

Sample Preparation

The fibers were first washed with different solvents to remove the sizing agents. Coupons were then prepared using these fibers with three different thicknesses of epoxy coating. In addition, samples were also prepared using original fibers with the sizing agent intact. After curing in ambient temperature for 7 days, the coupons were divided into two groups and placed in seawater and the deicing salt solution for 24 h. The coupons were then taken out of the solutions and dried out with a clean cloth. The back (glass sheet) and edges (carbon fibers) of each sample were painted with nickel print, which formed a conductive layer to facilitate the electrical connection to the carbon fibers. After 12 h, the nickel print was dry and the coupons were ready for testing. Immediately before each experiment, the surface of the steel specimens were smoothed with grit 80 sandpaper and then polished with

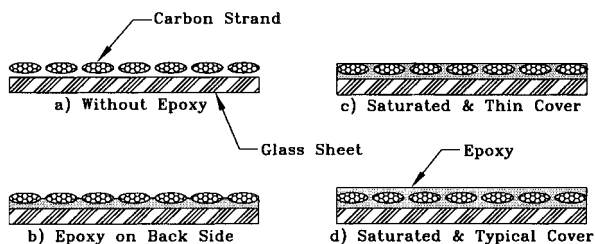


FIG. 6. Carbon Composite Samples with Different Amount of Epoxy Coating

grit 150 to ensure a uniform and reproducible surface each time.

Experimental Setup

All electrochemical measurements were performed on an EG&G Princeton Applied Research 273A Potentiostat/Galvanostat. The complete setup is shown in Fig. 7. Both potentiodynamic polarization tests and galvanic corrosion tests were carried out in a flat cell made from perfluoroalkoxy (PFA Teflon), as shown in Fig. 8. The cell had a volume of 100 mL with three openings that could be used for different electrodes, as displayed in Fig. 4 (polarization) and Fig. 5 (galvanic coupling). A standard O-ring was used to seal the specimens to

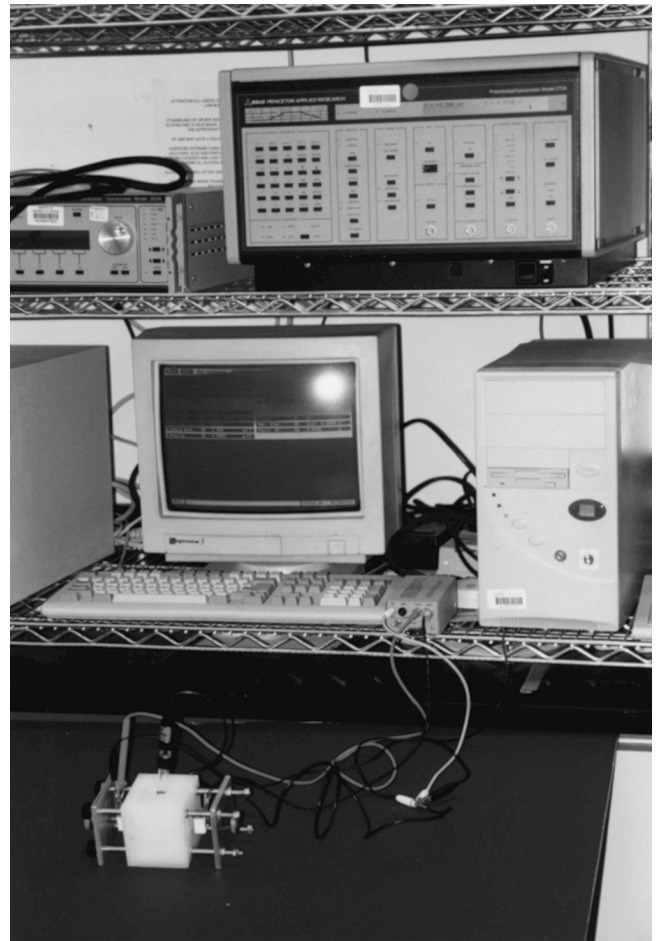


FIG. 7. Corrosion Test Setup

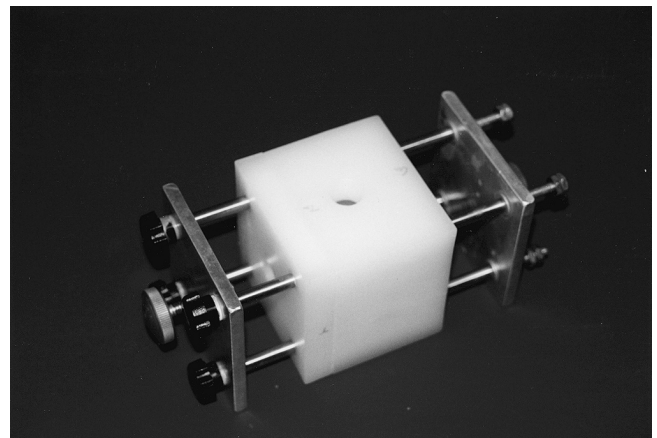


FIG. 8. Flat Cell Used in Corrosion Testing

TABLE 1. Test Matrix for Polarization Tests

Polarization test matrix	Seawater	Deicing solution
Steel	1	1
Carbon composite (thin epoxy coating)	1	1

TABLE 2. Test Matrix for Galvanic Coupling Tests

Fibers	Solutions		
(a) Part 1			
Washed fibers, seawater	Acetone	Isopropyl alcohol	Carbon tetrachloride
No epoxy	1	1	1
Epoxy on back	1	1	1
Thin epoxy coating	1	1	1
(b) Part 2			
As-received fibers	Seawater	Deicing solution	
No epoxy	1	1	
Epoxy on back	1	1	
Thin epoxy coating	1	1	
Typical epoxy coating	1	1	

the side openings while exposing exactly 100 mm² area of the specimen to the electrolyte.

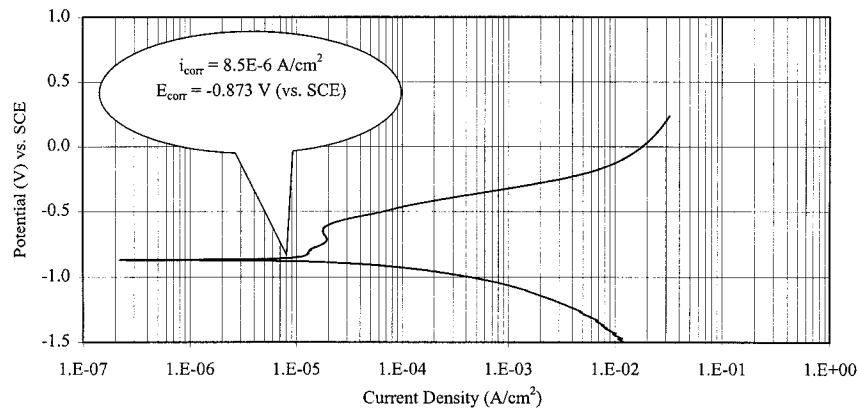
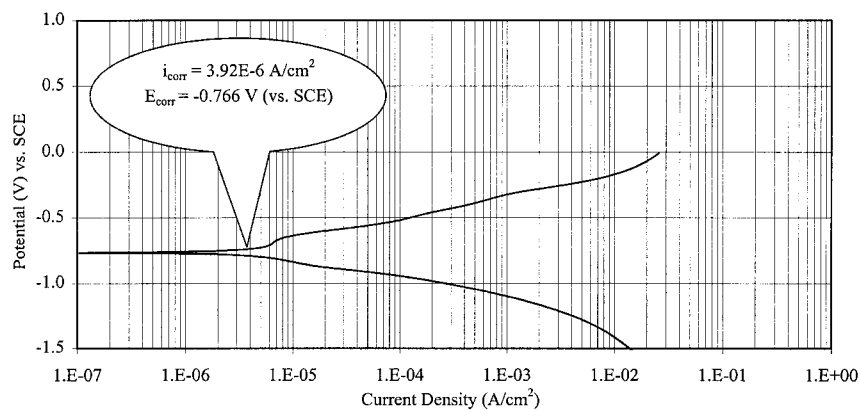
In the polarization tests, the working electrode was the specimen (steel or CFRP), the counter electrode was a platinum plate, and the reference electrode was the SCE. The steady-state condition was achieved approximately by switching off the potentiostat (about 30 min on average). The potential at this stage is the free corrosion potential, E_{corr} . Scanning was then performed at the rate of 1 mV/s, from 1 V below E_{corr} to 1 V above E_{corr} . The potential and current were monitored and

recorded during this period and subsequently plotted. For the polarization tests, a total of four specimens were tested in seawater and deicing salt solution (two steel specimens and two carbon specimens made from as-received fibers with thin epoxy coating).

In the galvanic corrosion test, a steel coupon served as the working electrode, while the counterelectrode was a carbon specimen and the reference electrode was again the SCE. During this test, the potentials of the two electrodes relative to the reference electrode were monitored. After reaching the steady-state condition, the values of the potentials were identical, indicating that the measured current between the working and the counterelectrode was the corrosion current density. At first, eight samples made with the original fibers with four different amounts of epoxy coating were tested. They were coupled with steel in both solutions, and the corrosion current densities were obtained (after about 20 min on average) for each test. Subsequently, nine samples made of washed fibers and three different epoxy covers were tested. They were coupled with steel only in seawater, and the corrosion current densities were obtained. Tables 1 and 2 summarize the test matrix for the polarization and galvanic coupling tests, respectively.

EVALUATION OF RESULTS AND ANALYSIS

Four polarization tests were conducted on two steel specimens and two specimens of carbon fibers in their original form, saturated and covered with a thin film of epoxy in seawater and deicing salt solution. The average thickness of epoxy cover on the exposed face of the specimens was less than 0.1 mm. Polarization diagrams of these experiments are shown in Figs. 9–12. By determining the Tafel slopes of both branches of the diagram (cathodic and anodic) and intersecting them, the corrosion current density (i_{corr}) and corrosion poten-

**FIG. 9.** Polarization Curve for Steel in Deicing Solution**FIG. 10.** Polarization Curve for Steel in Seawater

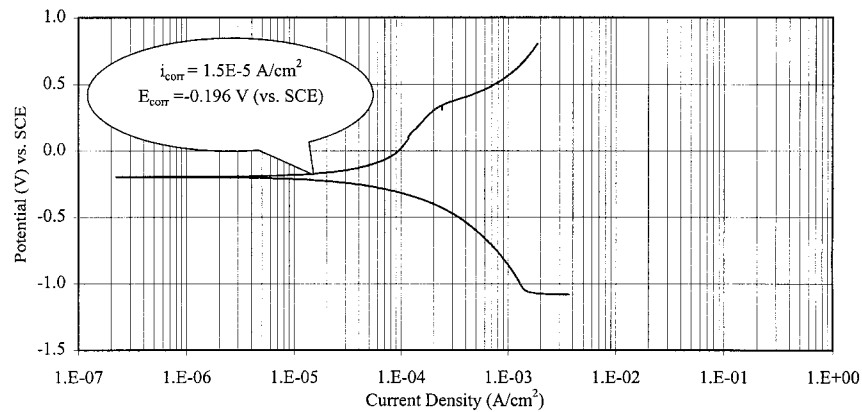


FIG. 11. Polarization Curve for Carbon Specimen with Thin Epoxy Coating in Deicing Solution

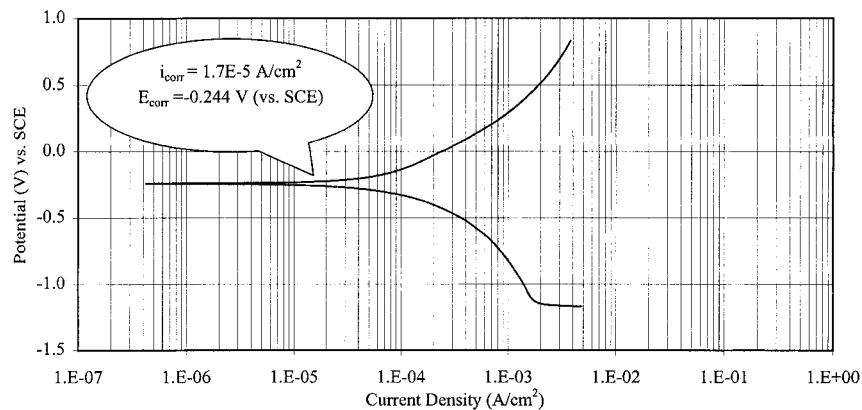


FIG. 12. Polarization Curve for Carbon Specimen with Thin Epoxy Coating in Seawater

tial (E_{corr}) of the individual material in a specific solution can be evaluated. The Tafel plots deviated from linearity for small and large polarization, and the Tafel slopes were considered as the slopes of the linear portions of the two branches.

In Fig. 9, it is clear that steel in deicing salt solution showed a minor sign of passivation along the anodic segments. Passivation indicates a situation in which a metal is temporarily protected from further corrosion by a thin film of corrosion product on its surface. The rate of corrosion is proportional to the corrosion current density (through Faraday's law) obtained from these diagrams. For steel, the anodic reaction is the oxidation of the metal or corrosion. In the case of CFRP, the anodic reaction is the oxidation of carbon that causes the degradation of the composite. Considering the pH of the electrolytes (7.90 for deicing salt solution and 7.25 for seawater), the cathodic reaction for both materials is the reduction of oxygen and the formation of hydroxide ion (OH^-) on the surfaces.

The corrosion potentials of carbon specimens were higher than those of steel in both solutions. As shown in Figs. 9 and 10, steel corrosion potential in deicing salt solution and seawater were -0.873 and -0.766 V versus SCE, respectively. The CFRP corrosion potentials were -0.196 and -0.244 V versus SCE, as shown in Figs. 11 and 12, respectively. Therefore, the carbon is more "noble" than steel in both electrolytes.

Meanwhile, the corrosion current densities of CFRP were higher than those of steel in both solutions. As shown in Figs. 9 through 12, the CFRP corrosion current densities were 1.5×10^{-5} , 1.7×10^{-5} A/cm² compared to those of steel, which were 8.5×10^{-6} , 3.9×10^{-6} A/cm² in deicing salt solution and seawater, respectively.

Steel tends to corrode faster when coupled with carbon in these solutions. The plots of steel and carbon for each solution were superimposed, as shown in Figs. 13 and 14. In order to

estimate the corrosion rate of the steel when coupled with carbon in each solution, the intersection of the two polarization plots of carbon and steel in the same solution on the Evans diagram was found. In both cases, the anodic polarization curves for steel (corrosion of steel) intersect the cathodic polarization curves for carbon (oxygen reduction on carbon). Corrosion current densities, i_{corr} , for the coupled systems were determined as 2.06×10^{-4} and 2.27×10^{-4} A/cm² for deicing salt solution and seawater, respectively. The values of i_{corr} for steel in deicing salt solution and seawater using Figs. 9 and 10 were 1.5×10^{-5} and 1.7×10^{-5} A/cm², respectively. Therefore, when coupled with carbon, steel corroded 13.7 and 13.4 times faster in the deicing salt solution and seawater, respectively, than in the absence of carbon. In both solutions, hydroxide ions were formed around carbon fibers inside the matrix as a byproduct of oxygen reduction.

For a more accurate measurement of the corrosion rate, galvanic corrosion tests were also performed. This was accomplished in two stages. The effects of different types of CFRP for the two solutions were examined. By testing four pairs of carbon specimens with different thicknesses of epoxy coating in deicing salt solution and seawater, both parameters (thickness of epoxy coating and type of solution) were investigated. The results of the galvanic corrosion tests are shown in Fig. 15. After 1,000 s, all the experiments reached steady state, and the galvanic current density of each test was obtained. The galvanic corrosion current density for the steel coupled to carbon specimens with the thin film of epoxy coating were 0.93×10^{-4} and 0.85×10^{-4} A/cm² in deicing salt solution and seawater, respectively. These values were confirmed by the results of the polarization tests shown in Figs. 13 and 14 (2.06×10^{-4} and 2.27×10^{-4} A/cm² in deicing salt solution and seawater, respectively).

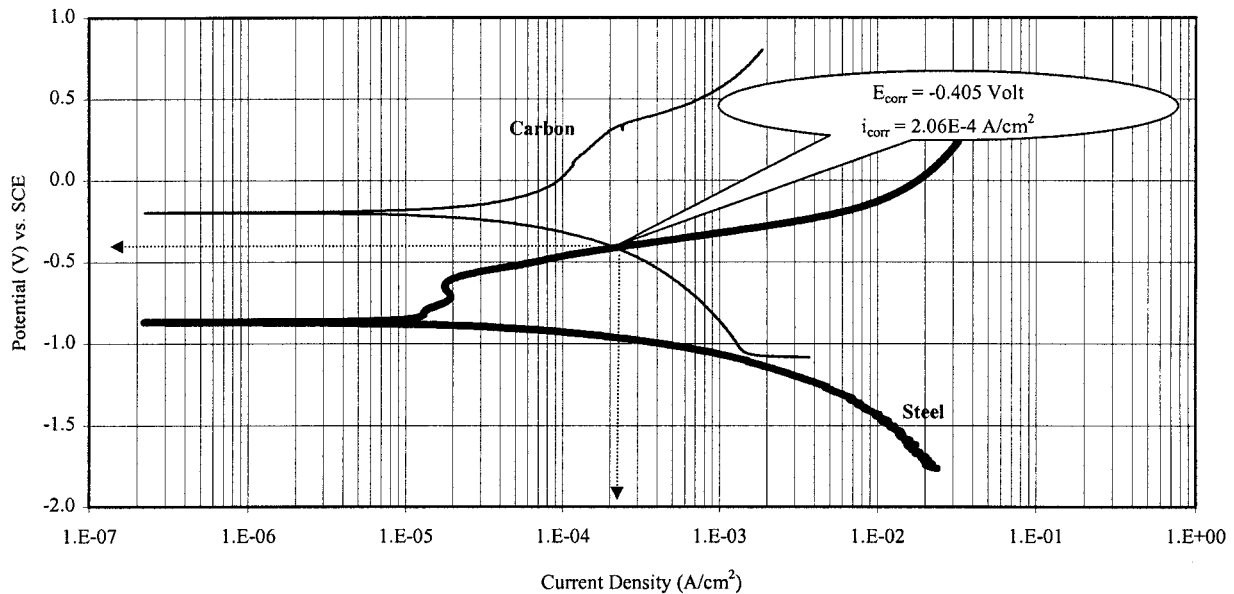


FIG. 13. Evans Diagram for Carbon Composite with Thin Epoxy Coating in Deicing Solution

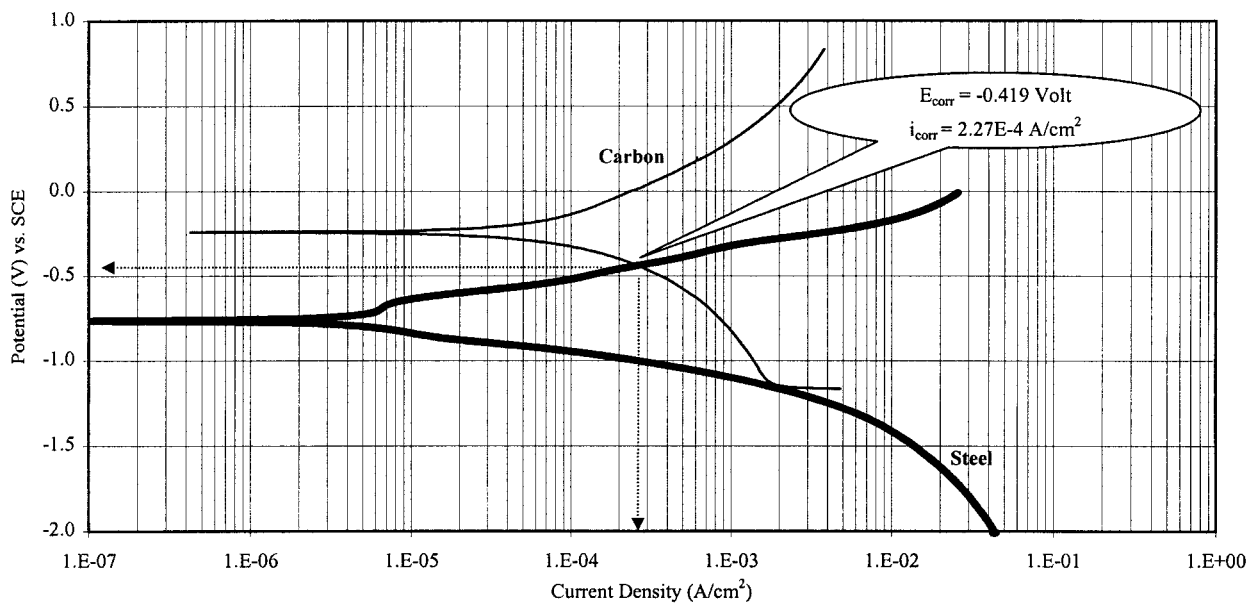


FIG. 14. Evans Diagram for Carbon Composite with Thin Epoxy Coating in Seawater

Effect of Epoxy Coating

Considering the results shown in Fig. 15, the effect of the epoxy coating on the carbon specimens was very pronounced. When the thickness of the epoxy increased, the corrosion rate for steel decreased. In seawater, a decrease in corrosion rate from 3.77×10^{-4} A/cm² for the bare fibers to 1.8×10^{-5} A/cm² for the coated fibers with an average coating thickness of 0.25 mm, as commonly used in practice, was observed. Even for a thin film of the epoxy coating with average thickness of 0.1 mm, the corrosion rate decreased to 8.5×10^{-5} A/cm². In the deicing salt solution, a decrease in corrosion rate from 4.69×10^{-4} A/cm² for the bare fibers to 2.0×10^{-5} A/cm² and 9.3×10^{-5} A/cm² was observed for the fibers with an average coating thickness of 0.25 and 0.1 mm, respectively.

Steel, when coupled with carbon, showed a faster corrosion rate in both solutions. In contrast to the corrosion rates noted in Figs. 9 and 10, when coupled with carbon in seawater, the rate increased from 3.9×10^{-6} A/cm² to 1.8×10^{-5} A/cm² (0.25 mm coating), 8.5×10^{-5} A/cm² (0.10 mm coating), and 3.77×10^{-4} A/cm² (bare fibers). Analogously, in a deicing

solution the above rates increased from 8.5×10^{-6} to 2.0×10^{-5} A/cm² (0.25 mm coating), 9.3×10^{-5} A/cm² (0.10 mm coating), and 4.69×10^{-4} A/cm² (bare fibers).

Effect of Electrolyte

As shown in Fig. 15, the corrosion current densities are fairly similar in both deicing salt solution and seawater. The deicing salt solution exhibited a slightly higher rate of corrosion, especially for carbon fibers without epoxy coating or with a thin layer of epoxy on the backside only. The values of the galvanic corrosion rates for the specimens with the thin film of epoxy coating confirmed the results of the polarization tests shown in Figs. 13 and 14. Table 3 presents a summary of these results.

Effect of Solvents

The effectiveness of different solvents in removing the sizing agents from the surface of the fibers was also investigated. The corrosion current densities achieved at the end of each

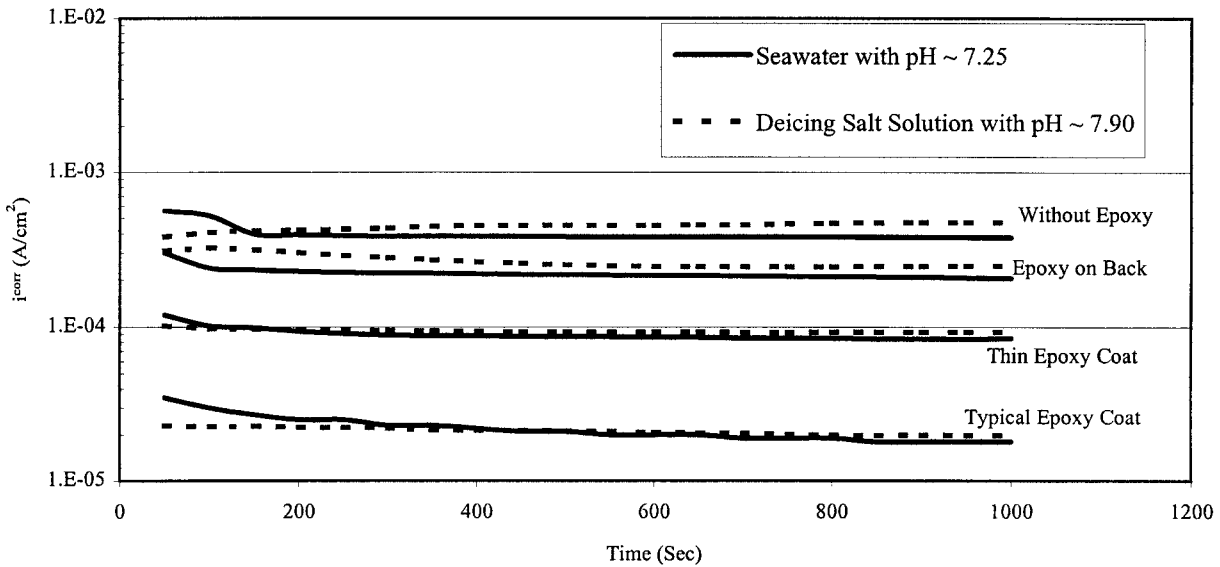


FIG. 15. Galvanic Coupling Results of Composite Made with Original Carbon Fibers and Steel in Seawater and Deicing Salt Solution

TABLE 3. Galvanic Current Densities of As-Received Fibers in Seawater and Deicing Solution

Solution	Galvanic Coupling ^a				Polarization ^a
	No epoxy	Epoxy on back	Thin epoxy coating	Typical epoxy coating	Thin epoxy coating
Seawater	3.77	2.05	0.85	0.18	2.27
Deicing salt	4.69	2.47	0.93	0.2	2.06

^aCurrent density (10^{-4} A/cm²).

test were recorded for the total of nine samples made of the carbon fibers washed with three different solvents. In this stage, three types of specimens were tested, and only seawater was considered as the electrolyte. As shown in Figs. 16–18, there was no significant change in the galvanic corrosion rate of the specimens made with fibers washed with those solvents. The results for the samples made with the as-received (intact) fibers showed similar corrosion current densities (with the same order of magnitude). Among the three solvents used, acetone was the most effective and increased the galvanic corrosion rate by 30 and 50% for samples without epoxy and with epoxy on the backside only, respectively. All washed fibers when covered with epoxy displayed much better resistance against galvanic corrosion. The galvanic current densities of these specimens were half those of the specimens made with as-received fibers. Table 4 presents a summary of these

results. The results also showed that the corrosion rate could be decreased by an order of magnitude by adding a thin layer of epoxy coating.

CONCLUSIONS

1. The test results indicate the existence of the galvanic corrosion when there is a direct contact between a CFRP laminate and steel substrate. The Evans diagram shows that when steel and carbon fibers coated with a thin film of epoxy are coupled together, the corrosion rate of steel increases by a factor of 24 and 57 in a deicing salt solution and seawater, respectively, for the specimens tested.
2. The galvanic corrosion rate is directly related to the epoxy coating thickness. Applying a thin film of epoxy coating (0.1 mm) on saturated carbon fibers decreases the galvanic corrosion rate in seawater and deicing salt solution by seven- and fivefold, respectively. By using saturated carbon fibers and thicker epoxy coating (0.25 mm, typical of that used in wet layup), the galvanic corrosion rate in seawater and deicing salt solution decreased by twenty-one- and twenty-threefold, respectively.
3. The galvanic corrosion rate in the deicing salt solution was slightly higher than that in seawater (15% on average). The difference was more pronounced for carbon fibers with no epoxy coating (24%).

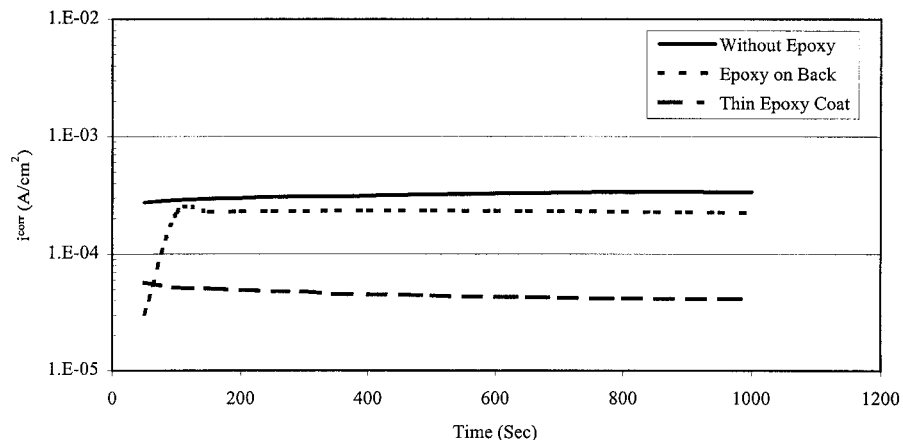


FIG. 16. Galvanic Coupling Results for Steel and for Carbon Fibers Washed with Carbon Tetrachloride in Seawater

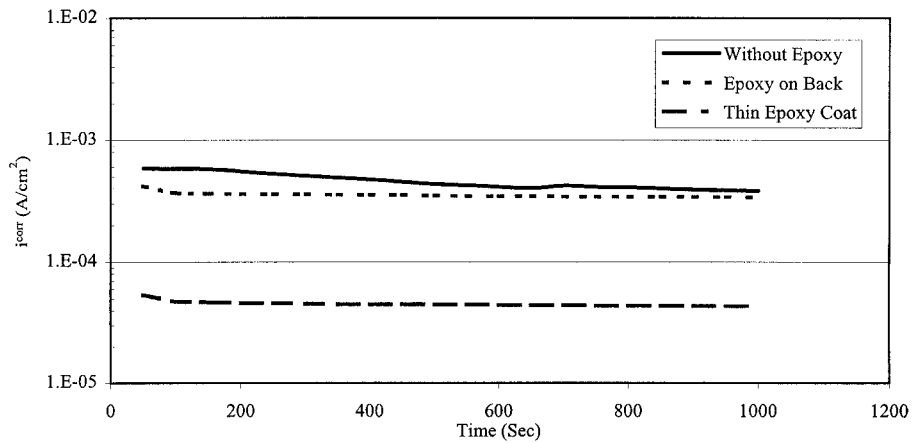


FIG. 17. Galvanic Coupling Results for Steel and for Carbon Fibers Washed with Isopropyl Alcohol in Seawater

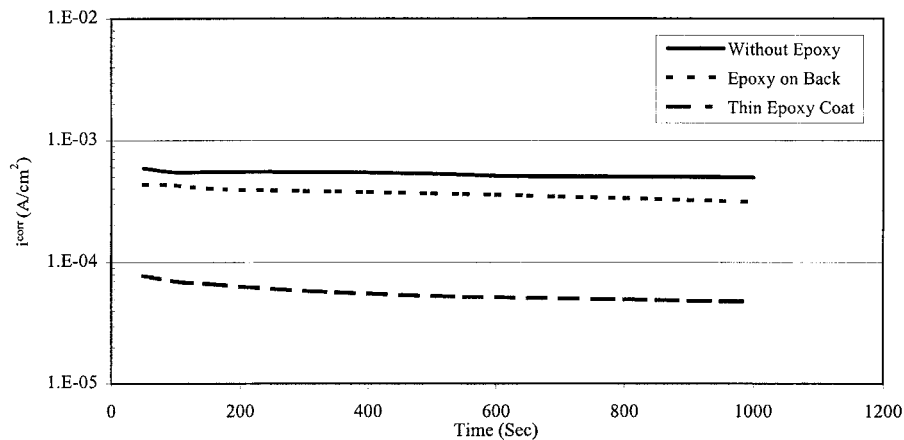


FIG. 18. Galvanic Coupling Results for Steel and for Carbon Fibers Washed with Acetone in Seawater

TABLE 4. Galvanic Current Densities of As-Received and Washed Fibers in Seawater

Seawater	As received ^a	Acetone ^a	Isopropyl alcohol ^a	Carbon tetrachloride ^a
No epoxy	3.77	4.96	3.84	3.36
Epoxy on back	2.05	3.12	3.39	2.24
Thin epoxy coating	0.85	0.48	0.44	0.42

^aCurrent density $\times 10^{-4}$ A/cm².

- Sizing agents decreases the galvanic corrosion rate of the carbon fibers. In the case of exposed fibers, acetone was the most effective solvent (50% change) for removing the sizing agents. The CFRP specimens made of washed fibers showed lower corrosion rates (50%).
- Considering the common cathodic reaction in CFRP laminates coupled with steel (the reduction of oxygen in solutions with pH > 7) and the evolution of hydroxide ions on the carbon fibers, the use of a matrix with hydrolyzable links (ester bonds) should be avoided in applications exposed to nonacidic deicing salt solution and seawater.
- Since the galvanic corrosion only initiates when there is direct contact between two dissimilar metals in the presence of an electrolyte, measures can be taken to eliminate one or both of these parameters and to eliminate this problem. The use of a nonconductive layer of fabric between carbon and steel, an isolating epoxy film on the steel surface, and a moisture barrier can be considered as a few preventive alternatives.

ACKNOWLEDGMENTS

The writers would like to acknowledge the funding of this research by the National Science Foundation, Grant No. CMS-9413857, with Dr. John B. Scalzi as program director. The results and conclusions presented here are those of the writers and do not represent the views of the National Science Foundation. The writers would like to thank Prof. Srin Raghavan of the Department of Material Science and Engineering at the University of Arizona for his help with this project.

REFERENCES

- Albrecht, P., Sahli, A., Crute, D., Albrecht, P., and Evans, B. (1984). "Application of adhesives to steel bridges." *Rep. No. FHWA-RD-84-037*, Federal Highway Administration, Washington, D.C., 106–147.
- ASTM. (1999). "Practice for preparation of substitute ocean water." *Annual book of ASTM standards, D 1141-98*, Vol. 11.02, West Conshohocken, Pa., 28–30.
- Cetin, K. M., Shaw, B. A., Bakis, C., Nanni, A., and Boothby, T. (1998). "Environmental degradation of repaired concrete structures." *Proc. 2nd Int. Conf. on Compos. in Infrastructures*, Vol. II, The University of Arizona, Tucson, Ariz., 488–500.
- Dusseck, I. J. (1980). "Strengthening of bridge beams and similar structures by means of epoxy-resin-bonded external reinforcement." *TRB Rec. 785*, Transportation Research Board, Washington, D.C., 21–24.
- Federal Highway Administration (FHWA) Bridge Program Group. (2000). *Count of deficient bridges by state non federal-aid highways as of June 30, 1998*, (<http://www.fhwa.dot.gov/bridges/britab.htm>), Washington, D.C.
- Fontana, M. G. (1987). *Corrosion engineering*, McGraw-Hill, New York.
- Klaiber, F. W., Dunker, K. F., Wipf, T. J., and Sanders, W. W. (1986). "Methods of strengthening existing highway bridges." *NCHRP Rep. No. 293*, Transportation Research Board, Washington, D.C., 1–40.
- Mertz, D. R., and Gillespie, J. W. (1996). "Rehabilitation of steel bridge girders through application of advanced composite material." *NCHRP Rep. No. 93-ID11*, Transportation Research Board, Washington, D.C., 1–20.

- Nara, H., and Gasparini, D. (1981). "Fatigue resistance of adhesively bonded connections." *Rep. No. FHWA-OH-81-001*, Federal Highway Administration, Washington, D.C., 125–135.
- Raithby, K. D. (1980). "External strengthening of concrete bridges with bonded steel plates." *Supplementary Rep. 612*, Dept. of Environment, Transport and Road Research Laboratory, Crowthorn, U.K., 16–18.
- Saadatmanesh, H. (1994). "Fiber composites for new and existing structures." *ACI Struct. J.*, 91(3), 346–354.
- Saadatmanesh, H., and Ehsani, M. R. (1991). "RC beams strengthened with GFRP plates. I: Experimental study." *J. Struct. Engrg.*, ASCE, 117(11), 3417–3433.
- Saadatmanesh, H., Ehsani, M. R., and Jin, L. (1997). "Repair of earthquake damaged RC columns with FRP wraps." *ACI Struct. J.*, 94(2), 206–215.
- Sen, R., and Liby, L. (1994). "Repair of steel composite bridge sections using carbon fiber reinforced plastic laminate." *Rep. No. 510616*, Florida Department of Transportation, Tallahassee, Fla.
- Sloan, F. E., and Talbot, J. B. (1992). "Corrosion of graphite-fiber-reinforced composites." *Corrosion*, 48(10), 830–838.
- Trethewey, K. R., and Chamberlain, J. (1988). *Corrosion for students of science and engineering*, Wiley, New York.
- Tucker, W. C., and Brown, R. (1989). "Blister formation on graphite/polymer composites galvanically coupled with steel in seawater." *J. Composite Mat.*, 23(4), 389–395.